(Received 20 February 2025, Accepted 29 April 2025, Scheduled 13 May 2025)

Design of a Miniaturized Circular Flower-Shaped Fractal Antenna with a Defected Ground Structure for Multiband Applications

Sanae Attioui[1], Asma Khabba[1,2], Saida Ibnyaich[1], Abdelouhab Zeroual[1], Zahriladha Zakaria[3], and Ahmed J. A. Al-Gburi[3,*]

[1]*Instrumentation, Signals and Physical Systems (I2SP) Team, Department of Physics Faculty of Sciences Semlalia, Cadi Ayyad University, Marrakech, Morocco*
[2]*LAMIGEP Laboratory, Moroccan School of Engineering Sciences (EMSI), Marrakech, Morocco*
[3]*Center for Telecommunication Research & Innovation (CeTRI), Fakulti Teknologi Dan Kejuruteraan Elektronik Dan Komputer (FTKEK), Universiti Teknikal Malaysia Melaka (UTeM), Jalan Hang Tuah Jaya, Durian Tunggal, Melaka 76100, Malaysia*

ABSTRACT: The increasing demand for compact, cost-effective, and versatile antennas in modern wireless communication systems has inspired research into innovative multiband antenna designs. However, numerous existing solutions are insufficient in terms of size, bandwidth, or manufacturing complexity, particularly when they aim to incorporate multiple wireless standards within a compact device. To address this gap, this study proposes a miniaturized fractal antenna design measuring $15 \times 11 \times 1.6\,\text{mm}^3$, fabricated on a low-cost FR-4 substrate. The proposed antenna is inspired by nature, featuring a flower-shaped patch and a defected ground (DGS) with a spiral pattern. It exhibits multiband behavior, resonating at six distinct frequencies: 1.79 GHz, 3.84 GHz, 7.34 GHz, 9.08 GHz, 11.44 GHz, and 14.6 GHz, making it suitable for various wireless applications, including GSM/UMTS (1.7–2.1 GHz), 4G/5G and radar (3.3–4.2 GHz), military radar and satellite communications (7–8 GHz), aviation and maritime radar (8.5–10 GHz), satellite communication in the Ku-band (10.7–12.7 GHz), and advanced radar and satellite uplinks (12–14 GHz). The fabricated antenna was tested, and the experimental results demonstrated a strong correlation with the simulated outcomes, confirming its practical applicability and effectiveness in multiband communication systems. The proposed fractal antenna stands out due to its compact size, multiband capability, and excellent performance, making it well suited for modern wireless applications.

1. INTRODUCTION

The rapid development of wireless communication systems has created a demand for antennas that can operate efficiently in multiple frequency bands while maintaining a compact and cost-effective design [1, 2]. Antennas ensure reliable multiband performance, which is crucial for wireless applications such as 5G, Wi-Fi, Internet of Things, and others [3], as well as for seamless connectivity across different frequencies [4, 5]. Traditional antenna designs are often limited by their size, bandwidth, and performances [6]. Innovative strategies have been explored to address these challenges [7], with fractal antenna designs emerging as a promising solution [8]. Fractal antennas have become a cutting-edge solution for multiband and wideband applications [9], as they are capable of operating at multiple frequencies with high efficiency and compactness [10], owing to their self-similar and space-filling properties [11, 12]. The intricate and efficient designs found in nature have long been a source of inspiration for technology [13, 14].

When fractal antenna designs are combined with a defective ground structure [15], the antenna performance is greatly increased, particularly for multiband operations [16]. These help improve antenna multifunctionality by achieving increased bandwidth [17], excellent impedance matching, and providing harmonic filtering [18]. This method is integrated seamlessly with the flexibility and compact size of fractal designs [19], allowing the development of highly efficient multiband antennas that are well suited for modern wireless communication systems [20]. The integration of these methods guarantees optimal performance across a broad frequency range [21, 22].

Multiband antennas are highly advantageous for the integration of multiple applications into a single device. There will be no requirement for multiple antennas once multiband operation is accomplished. The performance, miniaturization, and frequency adaptability of patch antennas are significantly enhanced by the incorporation of fractal geometry, which is a highly effective technique among various methods. Ref. [23] presents a multiband hybrid fractal antenna designed for public safety and 5G Sub-6 GHz bands. The radiating element integrates Koch and Hilbert fractal geometries on a multilayer FR4 substrate, $28 \times 60 \times 56\,\text{mm}^3$. The antenna resonates at 2.64 GHz, 3.87 GHz, 4.54 GHz, 5.02 GHz, 5.35 GHz, and 6.42 GHz, achieving gains from 0.9 to 4.6 dBi. In [24], a mi-

* Corresponding author: Ahmed Jamal Abdullah Al-Gburi (ahmedjamal@ieee.org, ahmedjamal@utem.edu.my).

crostrip fractal antenna is introduced which employs the DGS technique and rectangular fractal structures. It is fabricated on FR-4 epoxy with an overall dimension of $39.7 \times 47 \times 16\,\text{mm}^3$. Suitable for military, telecommunication, and C-band applications, it resonates at five multi-band frequencies within 2–8 GHz, including 2.10 GHz, 2.91 GHz, 4.32 GHz, 5.83 GHz, and 7.88 GHz, with a maximum gain of 1.92 dB. Ref. [25] shows an antenna designed using a modified Apollonian gasket fractal structure which has been optimized using an artificial neural network (ANN). It is constructed on an FR4 substrate with an overall dimension of $30 \times 30 \times 16\,\text{mm}^3$. The antenna is capable of operating at four resonant frequencies: 7.4 GHz, 8.2 GHz, 9.1 GHz, and 9.8 GHz, which are suitable for a variety of radar and wireless communication applications. The optimized gain reaches up to 4.5 dBi.

The need for antennas that can accommodate a wide range of frequency bands is on the rise as a result of the rapid expansion of small wireless devices. Antennas that are compact, affordable, and capable of operating across multiple bands are essential for contemporary communication systems, including satellite systems, 5G, and the Internet of Things. Many designs are either too large or lack a broad frequency range, despite advancements in fractal and DGS-based antennas. A small, inexpensive antenna with reliable multiband performance and impressive design is required for next-generation wireless systems.

This paper introduces a new miniaturized fractal antenna geometry inspired by natural phenomena. The design seamlessly integrates a flower-like shape into the patch structure, further enhanced by a rectangular whirl pattern to create a defected ground structure. Beyond its aesthetic appeal, this nature-inspired approach provides functional advantages, enabling the antenna to operate efficiently in multiband wireless applications. The miniaturized fractal antenna exhibits multiband behavior, resonating at six distinct frequencies: 1.79 GHz, 3.84 GHz, 7.34 GHz, 9.08 GHz, 11.44 GHz, and 14.6 GHz. Additionally, at 14.6 GHz, the antenna achieves a maximum gain of 6.58 dB. The proposed antenna is well suited for various wireless communication standards due to its optimized geometry, which facilitates resonance across a wide frequency range, as well as its compact size and excellent performance characteristics.

2. DESIGNS AND METHODOLOGY

2.1. Design Equations of the Circular Patch

The proposed antenna design starts with a conventional circular patch. Thickness of the substrate is dependent on the antenna's resonant speed, which establishes its gain. The thickness is selected within the range of $0.003\lambda_0 < h < 0.025\lambda_0$, where λ_0 is the wavelength at the resonant frequency, c the velocity of light ($c = 3 \times 10^8$ m/s), and f_r the resonant frequency. The substrate has a thickness of 1.6 mm at a frequency of 2.4 GHz. The antenna's efficacy is influenced by the substrate material, which is selected with a relative dielectric constant of $\epsilon_r = 44$ (FR4 material).

The radius of the circular patch, denoted as a, is calculated using the formula:

$$a = \frac{F}{\sqrt{1 + \frac{2h}{\pi\epsilon_r}\left[\ln\left(\frac{\pi F}{2h}\right) + 1.7726\right]}} \tag{1}$$

where

$$F = \frac{8,791 \times 10^9}{f_r\sqrt{\varepsilon_r}} \tag{2}$$

h is the height of the substrate. The effective dielectric constant of the substrate is then computed using the equation:

$$\varepsilon_{eff} = \frac{\varepsilon_r + 1}{2} + \frac{\varepsilon_r - 1}{2}\left(1 + \frac{12h}{a}\right)^{-\frac{1}{2}} \tag{3}$$

The length (L_{sub}) and width (W_{sub}) of the substrate are calculated using the expressions:

$$L_{\text{sub}} = 6h + 2a \tag{4}$$

$$W_{\text{sub}} = 6h + 2a \tag{5}$$

Ensuring that the substrate is sufficiently larger than the patch provides ample space for the fields to decay, thus reducing the effects of edge radiation and improving the antenna performance [26–29].

2.2. Proposed Antenna Geometry

The proposed fractal antenna features a distinctive design inspired by elements found in nature. With the inclusion of a flower-shaped structure within the circular patch, the design achieves an organic aesthetic. In addition, the antenna possesses a Defected Ground Structure that incorporates a rectangular whirl pattern, which enables it to operate efficiently at multiple frequency bands. The distinct and efficient antenna configuration is achieved through a combination of natural inspiration and innovative design. The suggested antenna is designed and fabricated using an FR4 substrate. This substrate has a permittivity of 4.4 and a tangent loss of 0.02. The dimensions of the antenna are $11 \times 15 \times 1.6\,\text{mm}^3$ and powered by a microstrip feedline with an impedance of 50 Ω. The evaluation of the antenna's characteristics and behavior was conducted through the utilization of ANSYS HFSS software. The final design of the proposed fractal antenna is depicted in Figure 1. In a similar vein, Figure 2 presents the prototype of the fabricated antenna, along with the accompanying measurement setup. In addition, the detailed dimensions of the proposed antenna can be found in Table 1.

2.3. Design Procedure

The initial design (Figure 3(a)) is a conventional circular antenna with a compact radius of 3.6 millimeters. In the second stage (Figure 3(b)), a set of circles is placed along the perimeter of the circular patch to start the flower design. Subsequently, in the third stage (Figure 3(c)), a set of circles is removed from the center of the circular patch to generate a flower-shaped patch, thereby creating an antenna inspired by nature and serving as

TABLE 1. Key parameters of the suggested fractal antenna.

Parameter	Value (mm)	Parameter	Value (mm)	Parameter	Value (mm)
W_s	11	L_s	15	W_g	11
L_{g1}	4	W_f	2	L_f	6.79
f_1	4.6	f_2	2.6	f_3	5
L_{g2}	3.75	L_{g3}	1	h_1	9.5
h_2	10	h_3	4	h_4	4.5
h_5	2.5	h_6	3	h_7	1
h_8	2	-	-	-	-

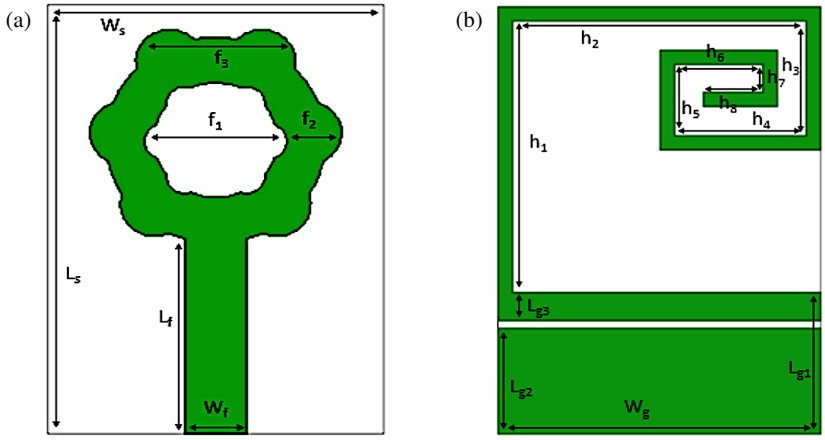

FIGURE 1. Geometry of the proposed fractal antenna, (a) top side and (b) bottom side.

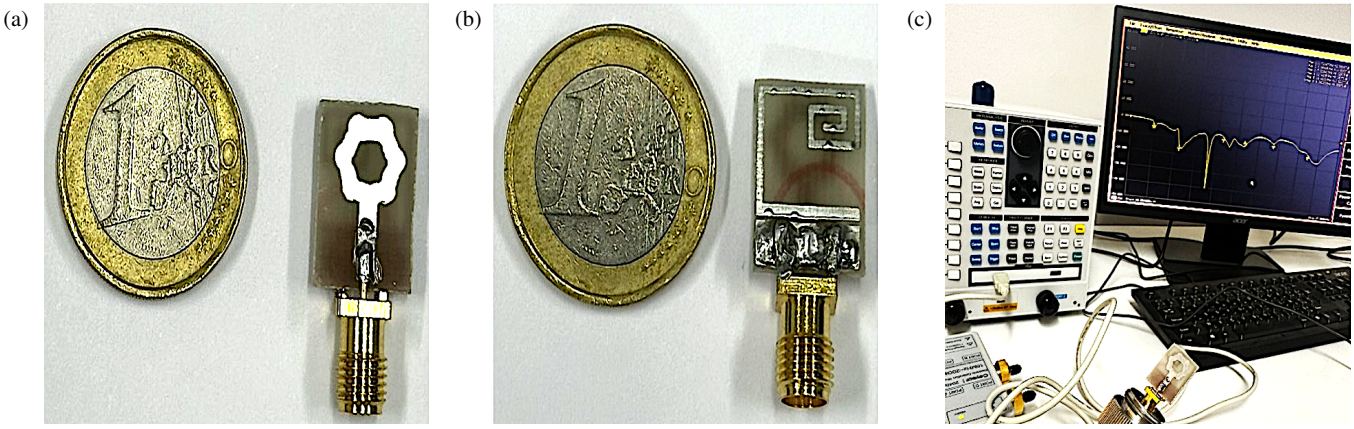

FIGURE 2. Fabricated prototype of the suggested antenna, (a) top side, (b) bottom side and (c) measurement setup.

a miniaturized antenna. The fourth step (Figure 3(d)) consists of adding a horizontal line, 11 mm long and 0.25 mm wide, to the initial partial ground, with the aim of introducing additional resonant frequencies. The fifth step (Figure 3(e)) involves incorporating additional resonant frequencies, achieved by introducing a vertical line to the partial ground. The final design (Figure 3(f)), a Defected Ground Structure with an incorporated rectangular whirl pattern, is intended to achieve multiple resonant frequencies, thereby facilitating the creation of a multi-band antenna. This design, inspired by natural principles, exhibits six resonant frequencies, allowing its utilization in various wireless applications.

Figure 4 shows the simulated reflection coefficient of the proposed fractal antenna across its six-step development process. The first stage presents two distinct resonance frequencies, which are 8.2 GHz and 14 GHz. The second step also presents two resonant frequencies, with a small gap between the resonant frequencies and the improved bandwidth. The third step displays two resonant frequencies, 8 GHz and 13.8 GHz, with a miniaturized antenna and an improved reflection co-

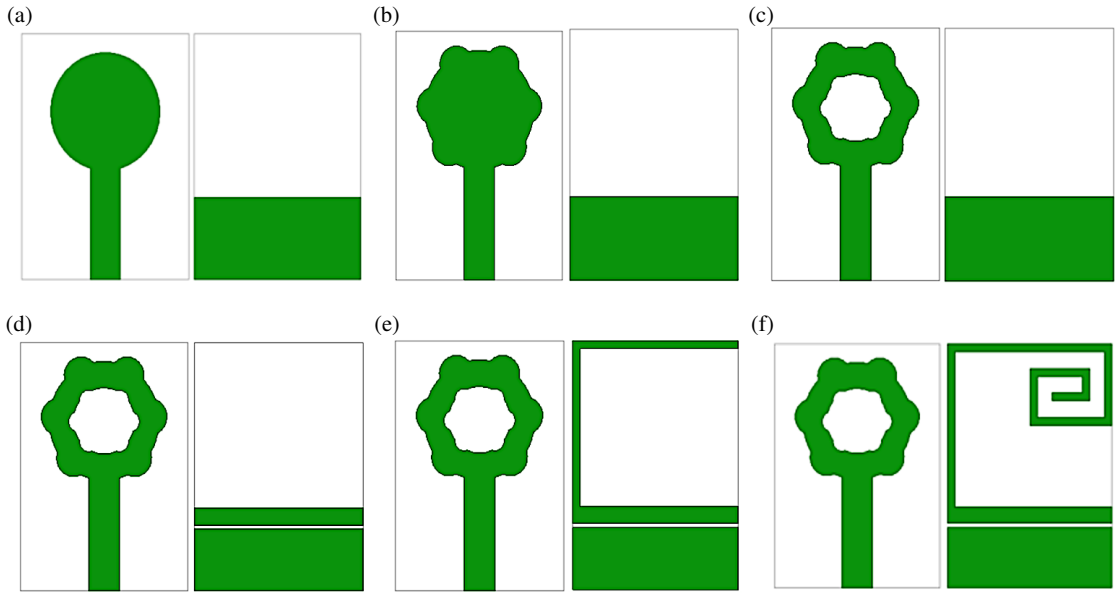

FIGURE 3. Illustration of the design evolution of the antenna, depicting its development from the initial basic structure to the final suggested configuration.

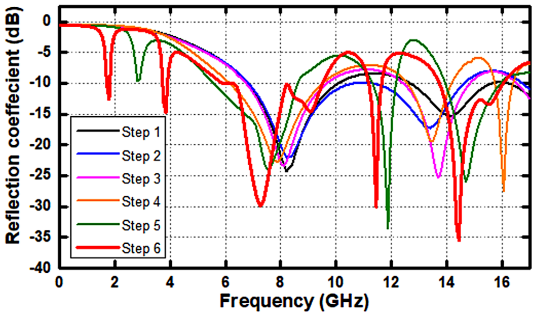

FIGURE 4. Simulated reflection coefficient of the proposed fractal antenna for the six steps.

efficient. The fourth stage introduces additional resonance frequencies of 7.96 GHz, 13.7 GHz, and 16 GHz, which confirms the multi-band behavior of the proposed fractal antenna. The fifth step presents four resonant frequencies: 2.8 GHz, 7.79 GHz, 11.97 GHz, and 14.6 GHz, exhibiting a favorable reflection coefficient and improved bandwidths. The final step highlights the multi-band performance of the proposed fractal antenna, which features six resonant frequencies: 1.79 GHz with a 100 MHz bandwidth, 3.84 GHz with a 120 MHz bandwidth, 7.34 GHz with a 1.88 GHz bandwidth, 9.08 GHz with a 1.36 GHz bandwidth, 11.44 GHz with a 530 MHz bandwidth, and 14.6 GHz with a wide 2.34 GHz bandwidth.

2.4. Parametric Analysis of the Proposed Antenna

A parametric analysis has been conducted on several variables that constitute the proposed fractal antenna, with the impact of each variable on the reflection coefficient presented graphically. The main objective of this study is to identify the key design elements necessary to maximize the reflection coefficient. This will ensure that the antenna experiences minimal power loss due to reflections, ultimately improving its overall performance.

Figure 5 shows the variation of the length L_{g1} between the partial ground plane and full ground plane. It has been observed that the lowest reflection coefficient is achieved near the intended target frequency ranges when the ground plane is 5 mm in length. This implies that the impedance is more precisely matched at those frequencies, resulting in a reduction in power loss. In contrast, the reflection coefficients increase as the ground planes become longer, which leads to a decrease in system efficiency. Consequently, the required excellent performance within the frequency range of relevance is achieved by a 5-mm-long partial ground plane.

Figure 6 illustrates the impact of adjusting the length h_2 from 7 mm to 11 mm with a 0.5 mm increment on the reflection coefficient in the fifth phase to optimize the spiral pattern for improved antenna performance. Upon completion of the figure analysis, the optimal length was $h_2 = 11$ mm, which exhibited the highest reflection efficiency and three resonant frequencies.

3. EQUIVALENT CIRCUIT MODEL

The proposed multi-band fractal antenna and its frequency response are modeled using an equivalent circuit approach, as shown in Figure 7. The modeling process is carried out within the Advanced Design System (ADS) software environment. In this approach, the antenna is represented as a combination of multiple resonators connected in series, where each resonator is modeled as an individual RLC circuit [30]. The number of resonant modes can be adjusted by adding or removing these resonant units. For this particular design, which operates across six resonance frequencies, each frequency corresponds to a parallel RLC resonant unit. The capacitance (C_0) and inductance (L_0) represent the characteristics of the antenna

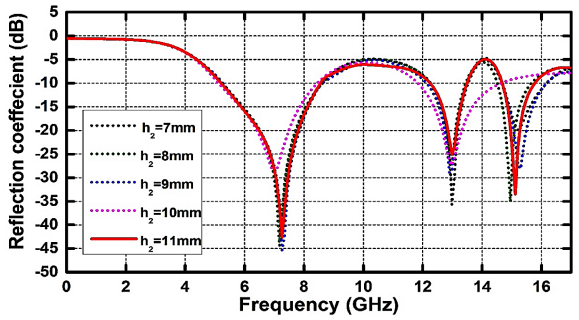

FIGURE 5. Effect of varying the length of L_g.

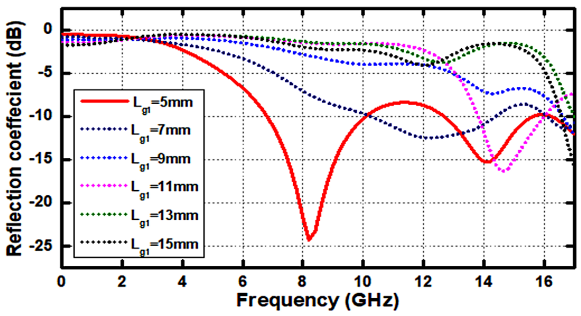

FIGURE 6. Effect of varying the length of h_2.

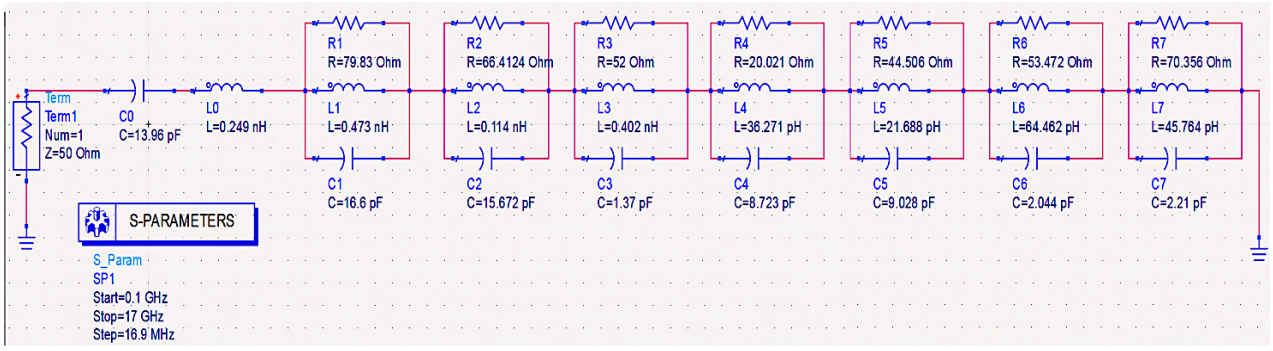

FIGURE 7. Equivalent circuit of the proposed circular fractal antenna.

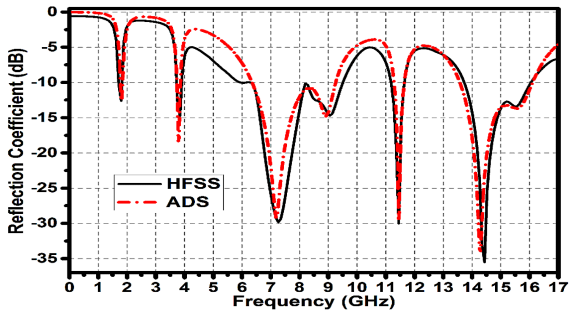

FIGURE 8. Simulated reflection coefficient of the circuit model with HFSS and ADS.

at its lowest resonant frequency. These lumped element values are optimized through simulation to achieve the best possible match with the reflection coefficient curve and its resonant peaks. The final optimized values for the lumped components are as follows: $C_0 = 13.96\,\text{pF}$, $L_0 = 0.249\,\text{nH}$, $R_1 = 79.83\,\Omega$, $L_1 = 0.473\,\text{nH}$, $C_1 = 16.6\,\text{pF}$, $R_2 = 66.412\,\Omega$, $L_2 = 0.114\,\text{nH}$, $C_2 = 15.672\,\text{pF}$, $R_3 = 52\,\Omega$, $L_3 = 0.402\,\text{nH}$, and $C_3 = 1.37\,\text{pF}$, $R_4 = 20.021\,\Omega$, $L_4 = 36.271\,\text{pH}$, and $C_4 = 8.723\,\text{pF}$, $R_5 = 44.506\,\Omega$, $L_5 = 21.688\,\text{pH}$, and $C_5 = 9.028\,\text{pF}$, $R_6 = 53.472\,\Omega$, $L_6 = 64.462\,\text{pH}$, and $C_6 = 2.044\,\text{pF}$, $R_7 = 70.356\,\Omega$, $L_7 = 45.764\,\text{pH}$, and $C_7 = 2.21\,\text{pF}$. As depicted in Figure 8, the reflection coefficient simulations conducted using both HFSS and ADS show excellent agreement, particularly across the seven operating frequency bands.

4. RESULTS AND DISCUSSIONS

In this section, the results are presented in terms of the antenna performance metrics, including reflection coefficient, input impedance, surface current distribution, radiation pattern, and gain. These factors clearly demonstrate that the constructed antenna will effectively provide proper impedance matching, resonant behavior, and directional properties, as required for its intended purpose.

4.1. Reflection Coefficient

Figure 9 illustrates the reflection coefficients for both measured and simulated data, therefore displaying the multi-band behavior of the proposed fractal antenna. The measured resonant frequencies, 2.1 GHz, 4.2 GHz, 7.54 GHz, 9.08 GHz, 11.44 GHz, and 14.6 GHz pretty closely match the simulated ones at 1.79 GHz, 3.84 GHz, 7.34 GHz, 9.08 GHz, 11.44 GHz, and 14.6 GHz. The corresponding -10 dB bandwidths for the measured and simulated results, respectively, are 260 MHz and 210 MHz at 2.1 GHz and 1.79 GHz, 260 MHz, and 220 MHz at 4.2 GHz and 3.84 GHz, 500 MHz and 380 MHz at 7.54 GHz and 7.34 GHz, 500 MHz and 400 MHz at 9.08 GHz, 500 MHz and 400 MHz at 11.44 GHz, and 900 MHz and 650 MHz at 14.6 GHz. The proposed antenna design's accuracy is confirmed by the close agreement between the measured and simulated findings, despite the presence of minor discrepancies that may be attributed to fabrication tolerances, material losses, and measurement setup restrictions.

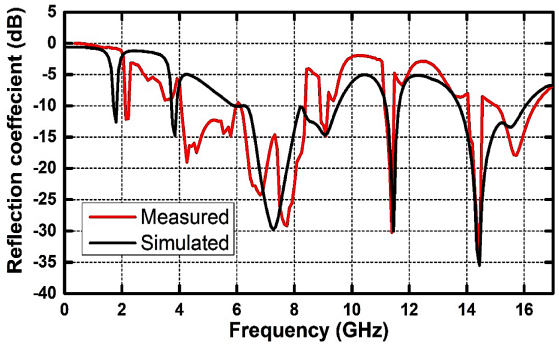

FIGURE 9. Measured vs simulated reflection coefficient of the proposed fractal antenna.

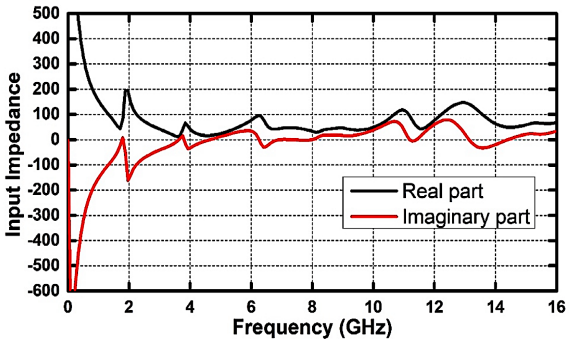

FIGURE 10. Input impedance of the proposed fractal antenna.

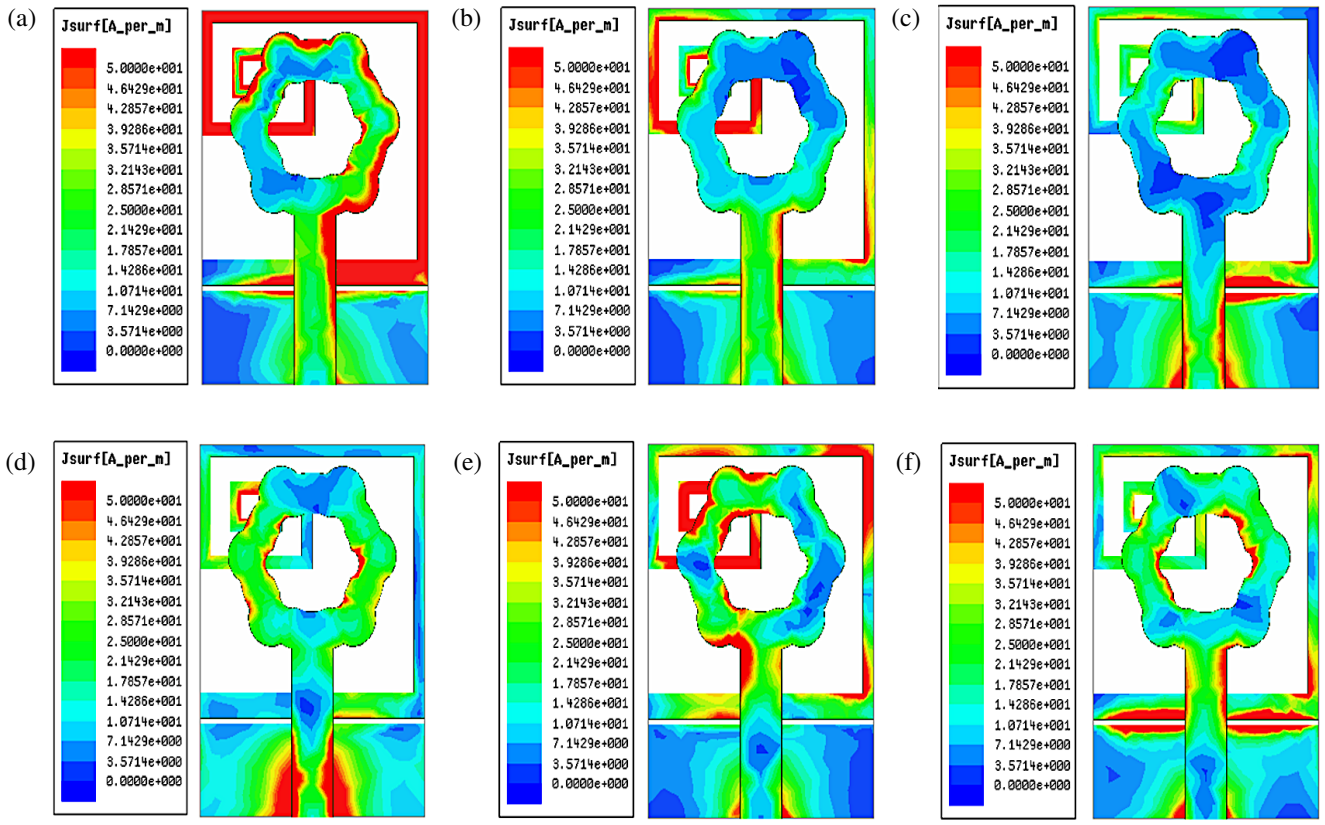

FIGURE 11. Surface current distribution of the proposed fractal antenna at frequencies: (a) 1.79 GHz, (b) 3.84 GHz, (c) 7.34 GHz, (d) 9.08 GHz, (e) 11.44 GHz, (f) 14.6 GHz.

4.2. Input Impedance

In the design of an antenna, the feed impedance is the most critical parameter, as it controls the transfer of power from the source to the antenna. The input impedance simulation results for the designed antenna are illustrated in the graph in Figure 10. The figure demonstrates that the input impedance, as simulated, has values that are nearly zero for the imaginary part and close to 50 Ω for the real part at the resonant frequencies. This aligns with the standard impedance value of the feed line. Adjusting the optimal parameters of the proposed antenna yields the impedance values that have been achieved.

4.3. Surface Current Distribution

The distribution of surface current at each resonant frequency is depicted in Figure 11. Alterations in areas with high current densities show that the distribution changes as the frequency changes, which could be due to resonant modes.

At 1.79 GHz, the surface current is concentrated near the whirl pattern and the edges of the flower-shaped structure, indicating a fundamental resonance mode. At 3.84 GHz, the current shifts upward and distributes along the structure's arms, indicating a higher order mode. The flower's outer edges develop hotspots with reduced central intensity at 7.34 GHz, revealing more complex resonance patterns. At 9.08 GHz, the current is

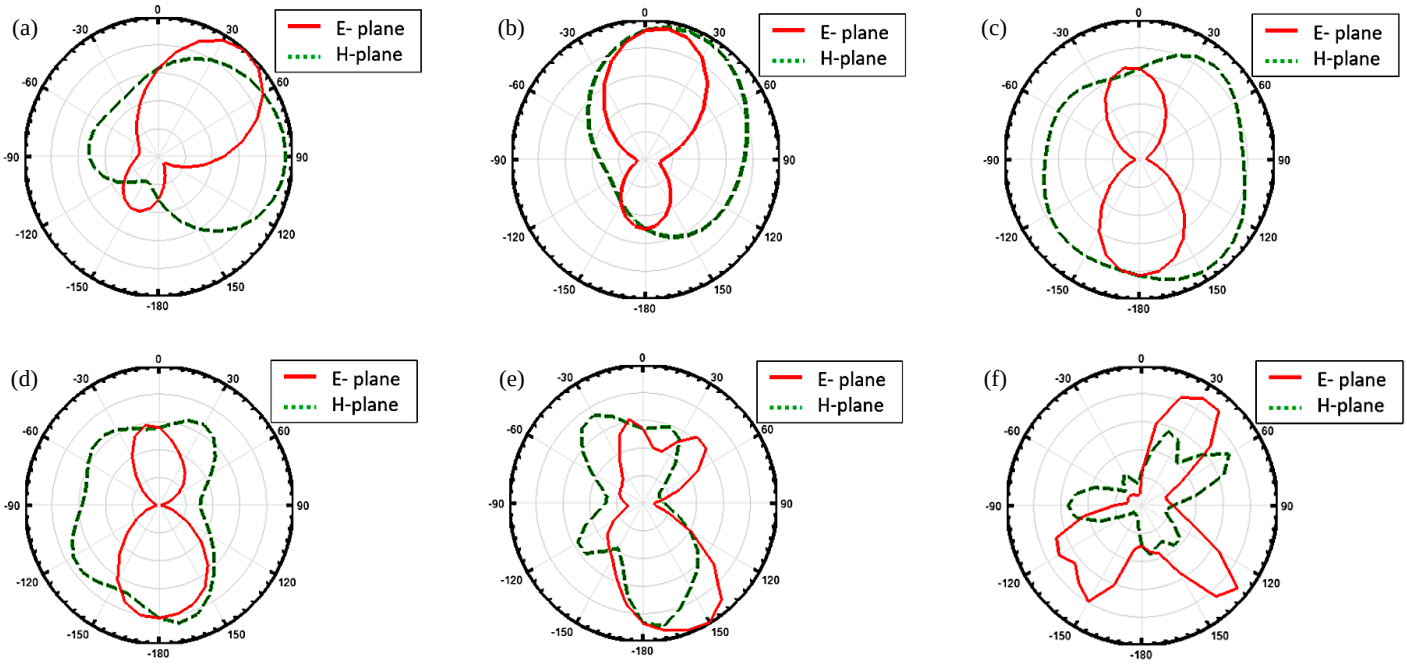

FIGURE 12. Simulated radiation pattern of the proposed fractal antenna at frequencies: (a) 1.79 GHz, (b) 3.84 GHz, (c) 7.34 GHz, (d) 9.08 GHz, (e) 11.44 GHz, (f) 14.6 GHz.

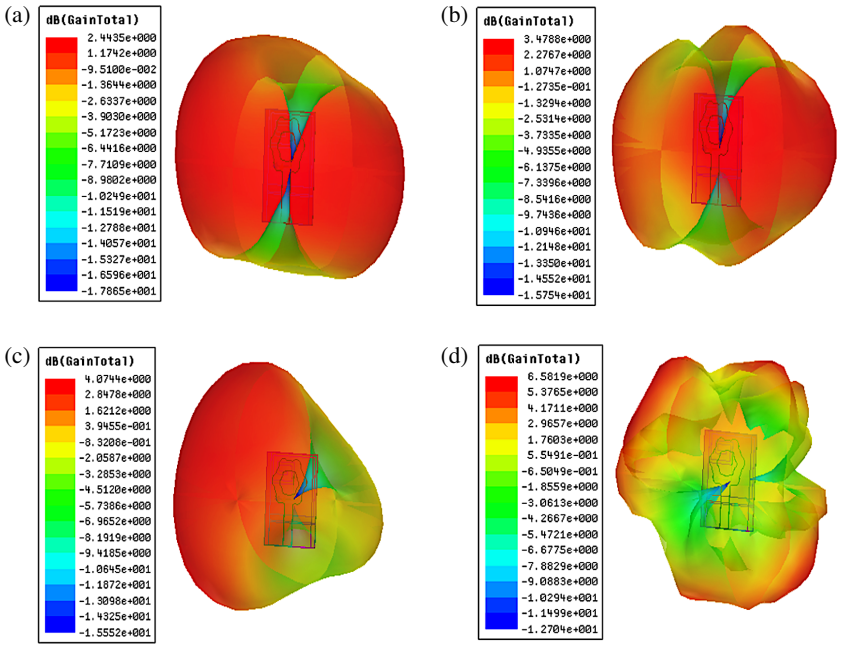

FIGURE 13. Gain of the proposed fractal antenna at frequencies: (a) 7.34 GHz, (b) 9.08 GHz, (c) 11.44 GHz and (d) 14.6 GHz.

more distributed in the edges of the whirl pattern. The flower's center is less active at 11.44 GHz, indicating higher-order resonance. Finally, at 14.6 GHz, the current concentrates along distant boundaries of the long line in the ground plane.

4.4. Radiation Pattern and Gain

Figure 12 illustrates the radiation patterns of the proposed antenna at the six resonant frequencies. Each plot illustrates the radiation characteristics of the E plane (electric field pattern) and H plane (magnetic field pattern). At 1.79 GHz, the radiation pattern is directional, with a strong forward lobe. Bidirectional lobes appear at 3.84 GHz. The patterns are bidirectional at 7.34 and 9.08 GHz, with more symmetry and lobes. The pattern shows multiple lobes with less symmetry at 11.44 GHz, indicating a more complex radiation mode. Finally, at 14.6 GHz, the pattern becomes irregular and multi-lobed, indicating radiation with multiple peaks. The 3D gain of the proposed antenna shown in Figure 13 reveals a substantial gain of 2.44 dB

TABLE 2. Comparison of the suggested fractal antenna with other antennas.

Reference	Size (mm^3)	Substrate material	Methodology Applied	Resonant Frequencies (GHz)	Maximum Gain
[2]	$87.5 \times 61 \times 1.6$	FR4	Triangle fractals	2.6, 3.8, and 5.3	3.34 dBi
[9]	$44.92 \times 45 \times 1.6$	FR4	Fractal shape	2.87, 6.39, 6.89, 8 and 8.51	8.87 dB
[10]	$27.84 \times 23.25 \times 1.6$	FR4	Descartes Circle Theorem	2.4 and 5.55	11.79 dBi
[6]	$35 \times 33 \times 1.6$	FR4	Annular circular rings	3.1 and 9.3	5.8 dBi
[7]	$34 \times 22 \times 1.57$	Rogers RT 5880	Slot in the patch	5.2, 6.6, 9, 12 and 13	7.7 dBi
[15]	$24 \times 40 \times 1.6$	FR4	DUMBBELL shaped	2.4, 2.7 and 7	3.98 dBi
[11]	$20 \times 18 \times 1.5$	FR4	Koch snowflake fractal	4, 8.5, 11.1, and 13.5	Not specified
Proposed antenna	$15 \times 11 \times 1.6$	FR4	Flower shaped with DGS	1.79, 3.84, 7.34, 9.08, 11.44 and 14.6	6.58 dB

at 7.34.5 GHz, 3.47 dB at 9.08 GHz, 4.07 dB at 11.44 GHz and 6.58 dB at 14.6 GHz. In itself, the antenna's exceptional gain is a criterion for selecting a high performing fractal antenna. Despite its compact and multi-band size, this design effectively leverages fractal geometry to achieve a high gain over a broad operating frequency range. The energy transfer is efficient, with minimal losses due to the low values of impedance mismatch and return loss. The embodiment of this antenna is indeed highly efficient, as evidenced by these characteristics. Consequently, it is a suitable choice for applications that require high-gain, wideband, and efficient operation.

4.5. Comparison of the Proposed Antenna with Other Antennas

The flower-shaped multi-band antenna is compared to other reported patch antennas in a detailed manner, as illustrated in Table 2. The comparison considers factors such as size, substrate material, bandwidth range, and resonance frequencies. The proposed circular fractal antenna is characterized by its exceptional capabilities, which are derived from nature and achieved through a compact form factor. This antenna is capable of providing exceptional performance and impressive bandwidth. With a particular emphasis on multi-band communication, this fractal multi-band antenna is highly effective in a variety of wireless applications. The proposed fractal antenna is well suited for modern multi-band applications, which is distinguished by its exceptional performance, multi-band behavior, and compact dimensions.

5. CONCLUSIONS

This paper presents an antenna inspired by nature, incorporating a fractal design, which offers a potential new approach to antenna development. Fractal antennas enhance bandwidth, miniaturization, and multi-band operation by utilizing intricate patterns and geometric self-similarity found in nature. The proposed fractal antenna features a circular patch shaped like a flower and a defected ground with a spiral pattern on the ground plane. The designed antenna was fabricated and evaluated, demonstrating satisfactory performance. It resonates at six distinct frequencies, making it compatible with a wide range of wireless applications, including GSM/UMTS, 4G/5G, and radar, as well as military radar, satellite communications, aviation and maritime radar (8.5–10 GHz), Ku-band satellite communication, and advanced radar and satellite uplinks. In addition to its substantial gain, the antenna's strong performance further reinforces its suitability for these applications.

ACKNOWLEDGEMENT

The authors would like to thank Universiti Teknikal Malaysia Melaka (UTeM) and the Ministry of Higher Education (MOHE) of Malaysia for supporting this project.

REFERENCES

[1] Elabd, R. H. and A. J. A. Al-Gburi, "Design and optimization of a circular ring-shaped UWB fractal antenna for wireless multi-band applications using particle swarm optimization," *Progress In Electromagnetics Research B*, Vol. 106, 101–112, 2024.

[2] Kumar, A., G. Singh, M. K. Abdulhameed, S. R. Hashim, and A. J. A. Al-Gburi, "Development of fractal 5G MIMO antenna for sub 6 GHz wireless automotive applications," *Progress In Electromagnetics Research M*, Vol. 130, 121–128, 2024.

[3] Bharti, G. and J. S. Sivia, "Koch curves and hexagonal ring-shaped geometry based ultra-wideband fractal antenna," *Wireless Personal Communications*, Vol. 137, No. 4, 2535–2555, 2024.

[4] Benkhadda, O., M. Saih, S. Ahmad, A. J. A. Al-Gburi, Z. Zakaria, K. Chaji, and A. Reha, "A miniaturized tri-wideband sierpinski hexagonal-shaped fractal antenna for wireless communication applications," *Fractal and Fractional*, Vol. 7, No. 2, 115, 2023.

[5] Aravindraj, E., G. Nagarajan, and P. Ramanathan, "A compact sierpinski gasket fractal antenna for S, C, X, and Ku band applications," *Progress In Electromagnetics Research C*, Vol. 141, 33–40, 2024.

[6] Aras, U., T. S. Delwar, P. Durgaprasadarao, P. S. Sundar, S. H. Ahammad, M. M. A. Eid, Y. Lee, A. N. Z. Rashed, and J.-Y. Ryu, "Dual features, compact dimensions and X-band appli-

cations for the design and fabrication of annular circular ring-based crescent-moon-shaped microstrip patch antenna," *Micromachines*, Vol. 15, No. 7, 809, 2024.

[7] Hassan, S. K. and Z. M. Khudair, "Circular patch antenna with quintuple band operation design analysis and performance evaluation for multi-frequency applications," *International Journal of Intelligent Engineering and Systems*, Vol. 17, No. 3, 671–681, 2024.

[8] Yadav, K., A. Jain, N. M. O. S. Ahmed, S. A. S. Hamad, G. Dhiman, and S. D. Alotaibi, "Retracted article: Internet of thing based koch fractal curve fractal antennas for wireless applications," *IETE Journal of Research*, Vol. 69, No. 10, V–XIV, 2023.

[9] Taniya, "Design and analysis of modified circular fractal antenna for S, C and X-band applications," *International Journal of Engineering Applied Sciences and Technology*, Vol. 5, No. 12, 169–175, 2021.

[10] Palanisamy, S., A. R. Vaddinuri, A. A. Khan, and M. Faheem, "Modeling of inscribed dual band circular fractal antenna for Wi-Fi application using descartes circle theorem," *Engineering Reports*, Vol. 7, No. 1, e13019, 2025.

[11] El Aoud, S. E., H. Abbaoui, O. Benkhadda, S. Attioui, N. E. Assri, S. Ibnyaich, A. Zeroual, M. M. Ismail, and A. J. A. Al-Gburi, "Design of a crescent moon-shaped reconfigurable patch antenna using a PIN diode for 5G sub-6 GHz and multistandard wireless applications," *Progress In Electromagnetics Research B*, Vol. 109, 81–93, 2024.

[12] Chrij, D., A. Khabba, Z. E. Ouadi, L. Sellak, J. Amadid, O. Benkhadda, S. Ibnyaich, A. Zeroual, and A. J. A. Al-Gburi, "A low-cost wideband SIW antenna with bilateral slots on FR4 epoxy for Ku-band applications," *Progress In Electromagnetics Research M*, Vol. 131, 61–70, 2025.

[13] Attioui, S., S. E. E. Aaoud, S. Ibnyaich, and A. Zeroual, "Minkowski fractal antenna design with defected ground structure for 5G millimeter wave applications," in *2024 International Conference on Global Aeronautical Engineering and Satellite Technology (GAST)*, 1–4, Marrakesh, Morocco, 2024.

[14] Al-Gburi, A. J. A., I. B. M. Ibrahim, Z. Zakaria, and N. F. B. M. Nazli, "Wideband microstrip patch antenna for sub 6 GHz and 5G applications," *Prz. Elektrotechniczny*, Vol. 97, No. 11, 26–29, 2021.

[15] Bhunia, S., K. Guha, and T. Tewary, "Hybrid shaped multiband microstrip patch antenna for wireless communication applications," *Journal of Nano- and Electronic Physics*, Vol. 16, No. 4, 04017, 2024.

[16] Sreenivasulu, M., E. K. Kumari, R. R. Reddy, and S. B. T. Abhyuday, "Minkowski fractal antenna with circular DGS for multiband applications," in *2022 IEEE Wireless Antenna and Microwave Symposium (WAMS)*, 1–5, Rourkela, India, 2022.

[17] Reha, A., O. Benkhadda, A. O. Said, A. E. Amri, and A. J. A. Al-Gburi, "Design of sub-6 GHz and sub-7 GHz dragon fractal antenna for 5G applications with enhanced bandwidth," *International Journal of Intelligent Engineering & Systems*, Vol. 18, No. 2, 14–22, 2025.

[18] Koteswara Rao Devana, V. N. and A. M. Rao, "A compact fractal dual high frequency band notched UWB antenna with a novel SC-DGS," *Analog Integrated Circuits and Signal Processing*, Vol. 107, No. 1, 145–153, 2021.

[19] Samsuzzaman, M., M. S. Talukder, A. Alqahtani, A. G. Alharbi, R. Azim, M. S. Soliman, and M. T. Islam, "Circular slotted patch with defected grounded monopole patch antenna for microwave-based head imaging applications," *Alexandria Engineering Journal*, Vol. 65, 41–57, 2023.

[20] Raj, A. and D. Mandal, "Design and analysis of sierpinski fractal antennas for millimeter-wave 5G and ground-based radio navigation applications," *Transactions on Emerging Telecommunications Technologies*, Vol. 35, No. 11, e70001, 2024.

[21] Sanugomula, M. and K. K. Naik, "A compact high gain circular shaped two-port MIMO antenna with fractal DGS for downlink satellite communication," *Progress In Electromagnetics Research M*, Vol. 125, 135–142, 2024.

[22] Varzakas, P., "Estimation of radio capacity of a spread spectrum cognitive radio rayleigh fading system," in *Proceedings of the 17th Panhellenic Conference on Informatics*, 63–66, Thessaloniki, Greece, 2013.

[23] Anand, S. and A. Kumar, "Multilayer multiband hybrid fractal antenna for public safety and 5G Sub-6 GHz bands," *Engineering Research Express*, Vol. 6, No. 3, 035346, 2024.

[24] Akkole, S. and N. Vasudevan, "Microstrip fractal multiband antenna design and optimization by using DGS technique for wireless communication," in *2021 6th International Conference on Inventive Computation Technologies (ICICT)*, 72–77, Coimbatore, India, 2021.

[25] Azzouz, A., R. Bouhmidi, and M. Chetioui, "Performance optimisation of modified multiband apollonian gasket fractal antenna using artificial neural network," *Microwave Review*, Vol. 30, No. 2, 54–59, 2024.

[26] Ibrahim, I. M., A. J. A. Al-Gburi, Z. Zakaria, and H. A. Bakar, "Parametric study of modified U-shaped split ring resonator structure dimension at ultra-wide-band monopole antenna," *Journal of Telecommunication, Electronic and Computer Engineering (JTEC)*, Vol. 10, No. 2-5, 53–57, 2018.

[27] Darimireddy, N. K., R. Nalanagula, R. Kumari, D. Z. Mohammed, Z. Zakaria, and A. J. A. Al-Gburi, "Wideband circularly polarized inverted cup shaped hybrid dielectric-resonator antenna over an asymmetric jerusalem cross-based metasurface," *Progress In Electromagnetics Research Letters*, Vol. 125, 59–66, 2025.

[28] Jetti, C. R., T. Addepalli, S. R. Devireddy, G. K. Tanimki, A. J. A. Al-Gburi, Z. Zakaria, and P. Sunitha, "Design and analysis of modified U-shaped four element MIMO antenna for dual-band 5G millimeter wave applications," *Micromachines*, Vol. 14, No. 8, 1545, 2023.

[29] Keriee, H. H., M. K. A. Rahim, N. A. Nayyef, Z. Zakaria, A. J. A. Al-Gburi, F. T. Al-Dhief, and M. M. Jawad, "High gain antenna at 915 MHz for off grid wireless networks," *Bulletin of Electrical Engineering and Informatics*, Vol. 9, No. 6, 2449–2454, 2020.

[30] Al-Gburi, A. J. A., I. M. Ibrahim, M. K. Abdulhameed, Z. Zakaria, M. Y. Zeain, H. H. Keriee, N. A. Nayyef, H. Alwareth, and A. D. Khaleel, "A compact UWB FSS single layer with stopband properties for shielding applications," *Przegląd Elektrotechniczny*, Vol. 2, No. 34, 165–168, 2021.